Sensitivity of the Polarization Ratio Method to Aerosol Concentration

Michelle G. Snyder*[a], Andrea M. Brown[b], and C. Russell Philbrick[a,c]

[a]Physics Department, North Carolina State University, Raleigh, NC 27695;
[b]John Hopkins Applied Physics Lab, Laurel, MD 20723; [c]Marine, Earth and Atmospheric Science Department, North Carolina State University, Raleigh, NC 27695

ABSTRACT

A multiwavelength, multistatic optical scattering instrument is being developed to characterize spherical aerosols. This instrument uses 405 nm (blue), 532 nm (green) and 655 nm (red) diode lasers and two CCD imagers to measure the angular distribution of light scattered from aerosols. The incident light is polarized parallel or perpendicular to the scattering plane; the scattered intensity is measured at backscatter angles ranging from 120° to 170° by CCD imagers. The phase function for each polarization is used to form the polarization ratio, which is used to characterize the aerosols. This method has proven to be a reliable way to characterize spherical aerosols by matching the measured polarization ratio with the polarization ratio calculated by the Mie scattering equations. This method is used to determine the number density, size distribution, and index of refraction of the aerosols. The sensitivity of the polarization ratio to particle concentration is explored using a narrow distribution of one micron polystyrene beads in a chamber. The aerosol concentration is found via an inversion technique that is based on Mie calculations. This study provides the basis for transitioning this instrument to measure multiple particle size ranges and concentrations for common aerosols in an outdoor environment.

Keywords: Aerosols, Aerosol Concentration, Polarization Ratio, Mie Scattering, Inversion

1. INTRODUCTION

Aerosols are one of the least well known components in climate forecasting models and influence surface solar radiation flux measurements. The multiwavelength multistatic technique is developed to take advantage of the optical scattering of spherical aerosols to determine their concentration, mean size and size distribution. This technique is based on matching scattered intensity data with Mie calculations for spherical particles. These calculations depend on the index of refraction and the size of the aerosol, as well as the polarization of the light incident on the aerosol. The larger the aerosol, or the smaller the wavelength, the more structure in the scattering. The value ka is used to represent this relationship, $ka = \frac{\pi * Diameter}{\lambda}$, thus as ka increases the structure increases as seen in Figure 1.

These angular phase functions are used to form the polarization ratio, which is defined as the intensity of the parallel polarized light divided by the perpendicular polarized light scattered at each scattering angle. The polarization of the incident light is referenced to the scattering plane formed by the axis of the laser beam and the imager. This particular instrument collects the backscatter intensity at angles between 120° and 175° because this region contains the most information in the polarization ratio, see Figure 2.

Figures 1 and 2 show the scattering from both polarizations and the polarization ratio. Scattered light is produced from both the aerosols of interest and the background light; the polarization ratio measured in an experiment is the total polarization ratio formed from the scattering by aerosols and molecules. The total polarization ratio is computed by summing the scattering contributed by each size of scatterer in the distribution weighted by the number in the distribution. The total phase function for the light scattered is the sum contributed by the aerosol distribution and the molecular background.

*mgsnyder@ncsu.edu

Laser Radar Technology and Applications XVI, edited by Monte D. Turner, Gary W. Kamerman,
Proc. of SPIE Vol. 8037, 80370K · © 2011 SPIE · CCC code: 0277-786X/11/$18 · doi: 10.1117/12.884206

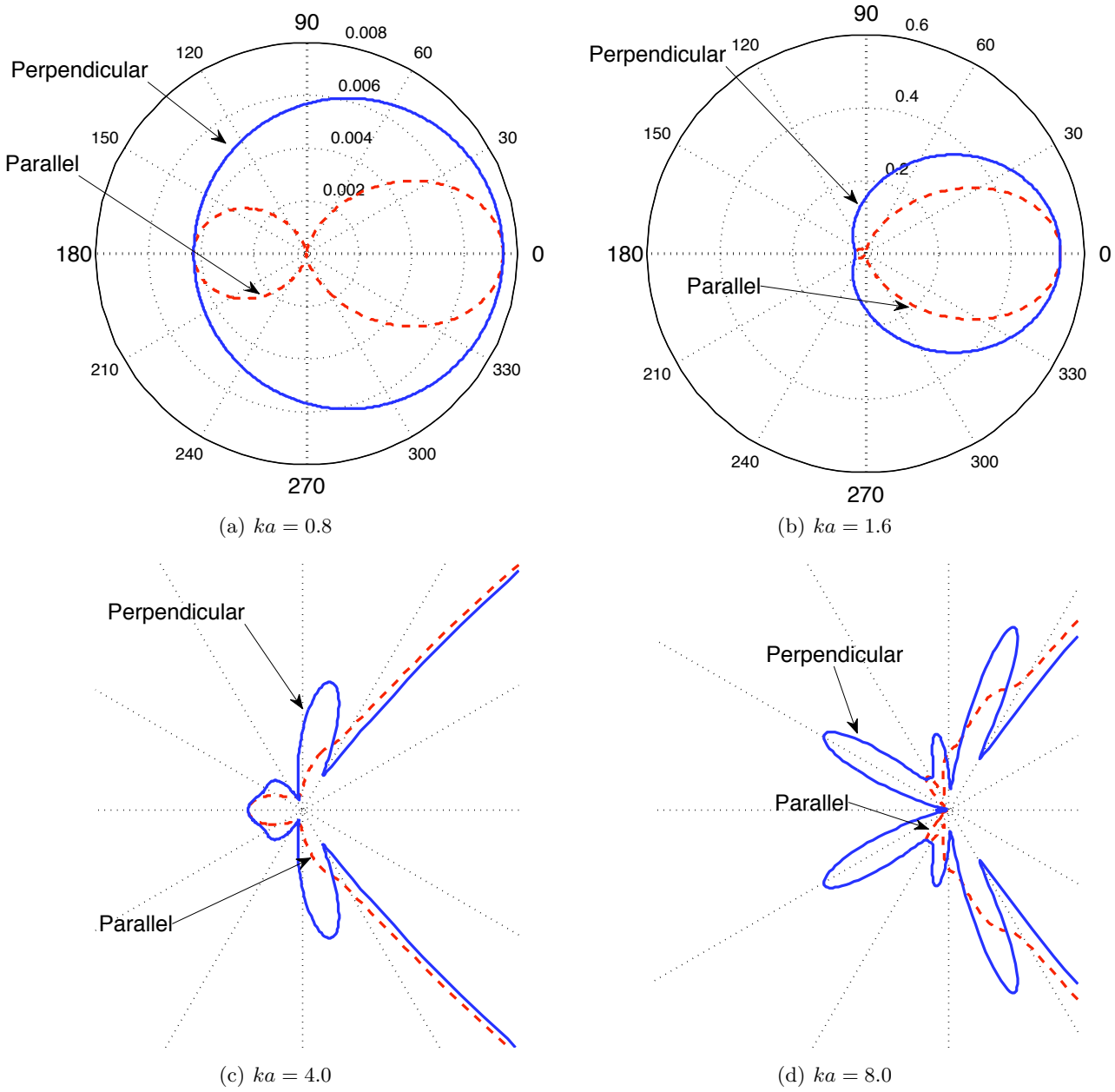

(a) $ka = 0.8$ (b) $ka = 1.6$

(c) $ka = 4.0$ (d) $ka = 8.0$

Figure 1. Angular scattering intensity as a function of ka, calculated using code from Bohren and Huffman.[1] The solid line is the perpendicular scattering component and the dashed line is the parallel scattering component (after Born and Wolf[2]).

The polarization ratio for a distribution of aerosol sizes is

$$PR(\theta) = \frac{I_{||}}{I_{\perp}} = \frac{\int N|S_2(x,\theta)|^2 y(x)dx + (2.54 \times 10^{19})S_{2molecules}(x,\theta)}{\int N|S_1(x,\theta)|^2 y(x)dx + (2.54 \times 10^{19})S_{2molecules}(x,\theta)}, \quad (1)$$

where S_2 is the scattering of the light polarized parallel to the scattering plane, S_1 is the scattering of the light polarized perpendicular to the scattering plane, N is the number concentration of aerosols, x is the size of the aerosol and $y(x)$ is the number of x size aerosols in the distribution.[3–6] From this equation it is obvious that as the concentration increases the contribution from the aerosols becomes greater than that of the molecular

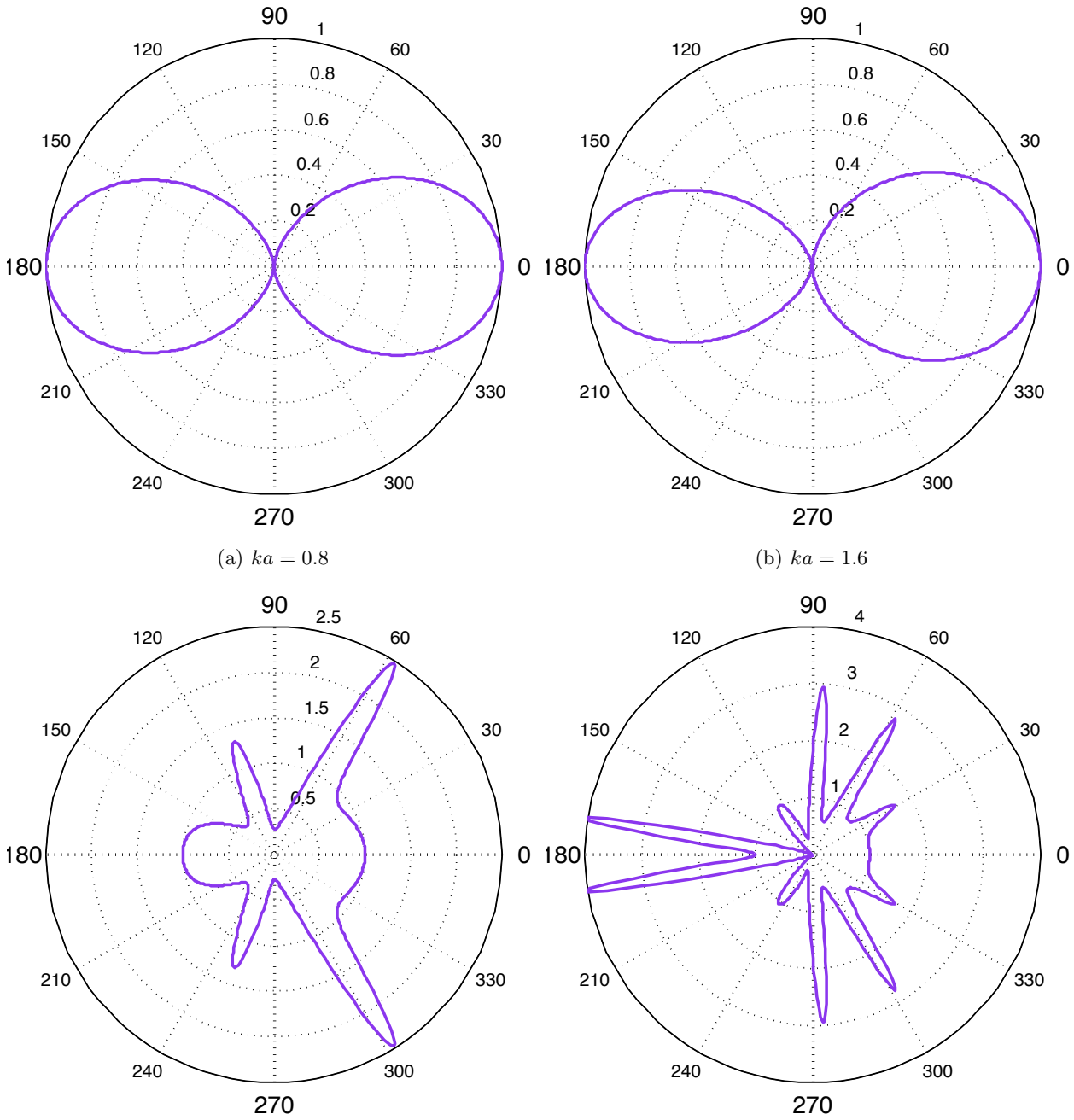

(a) $ka = 0.8$ (b) $ka = 1.6$

(c) $ka = 4.0$ (d) $ka = 8.0$

Figure 2. Plots demonstrate the behavior of the polarization ratio of horizontal (parallel) to vertical (perpendicular) phase functions at each angle.

background. Eventually the polarization ratio becomes dominated by the aerosols; thus, the polarization ratio technique is sensitive to the concentration of the aerosols. The following sections describe the instrument used to make measurements of the polarization ratio, the results from an experiment with one micron polystyrene latex (PSL) spheres.

2. INSTRUMENT

The transmitter consists of three lasers, necessary optics used to co-align the three wavelengths, and a broadband rotator at the end of the transmitter to control the polarization of the beam, see Figure 3. This rotator is remotely controlled to flip the polarization plane between a horizontal and a vertical orientation.

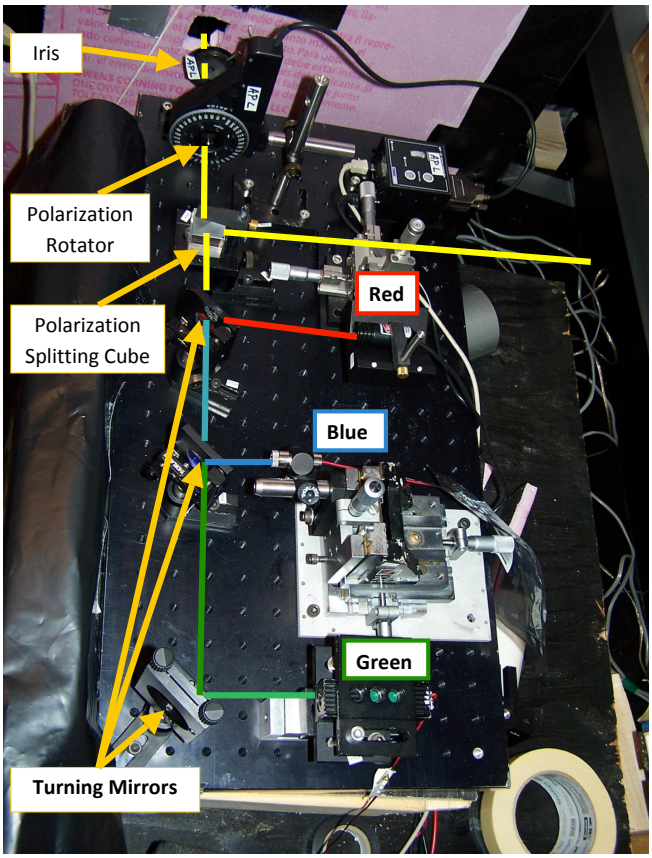

Figure 3. The transmitter consists of three co-aligned laser beams

The imager is located on the same horizontal plane as the beam, so the horizontal polarization plane is parallel to the scattering plane for these experiments. A diffraction grating is placed in front of the imager to spatiality separate the three scattered intensities by wavelength, see Figure 4. The first order diffracted lines are used to measure intensity versus scattering angle and are used to calculate the polarization ratio.

Alignment pictures are taken before the experiments are conducted; these use wire dangles at known distances in the beam, see Figure 5(a). The spatial distances between the dangles and the imager are measured to find the scattering angle that each pixel represents. The alignment picture is also locates the position of the first order diffracted beams, see Figure 5.

The measured polarization ratio is used as the input in the inversion routine to calculate the concentration, mean diameter, and standard deviation of the aerosol distribution. All aerosols are assumed to be spherical and have a size distribution described by the lognormal distribution. Several inversion routines have proven useful, including the binary genetic algorithm recently developed by Brown et al.[6,7] A more efficient inversion routine has also been tested, the continuous genetic algorithm. The continuous inversion routine is not limited by discrete numbers like the binary algorithm, and it demonstrates good results when compared to size distributions measured by an APS.

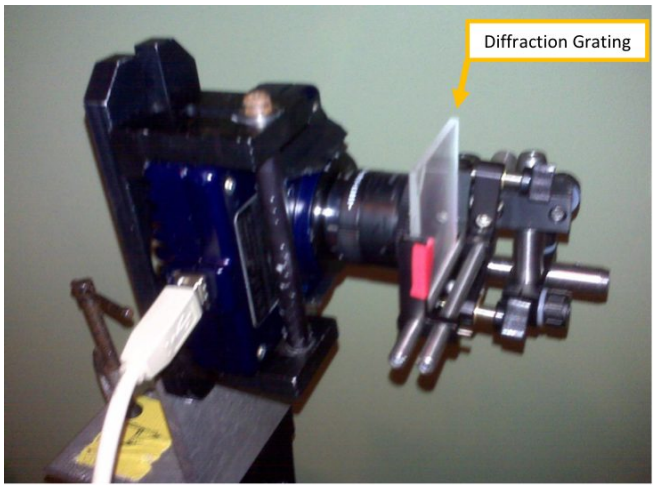

Figure 4. The imager has a diffraction grating mounted in front of the lens to spatially separate the beams in the image.

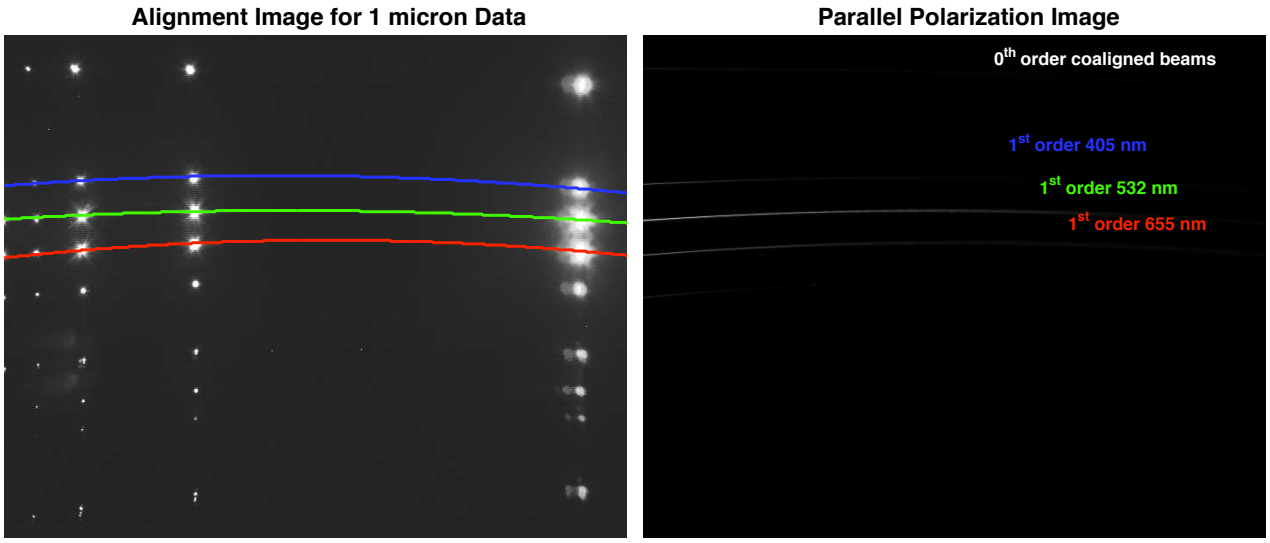

(a) Alignment Image (b) Diffracted Beams

Figure 5. An example of an alignment image used to locate the scattering angles for the first order diffraction of the there wavelengths.

3. INVERSION METHOD: POLARIZATION RATIO SENSITIVITY TO CONCENTRATION

The inversion routine is based on the polarization ratio from Mie calculations of the scattering phase functions, and use the index of refraction of the aerosols. The real and imaginary parts of the refractive index effect the phase functions and thus the polarization ratio; however, variation of the refractive index is not as significant as that of the concentration, mean diameter, or standard deviation. The effect due to the refractive index is shown in Figures 6(a) and 6(b).

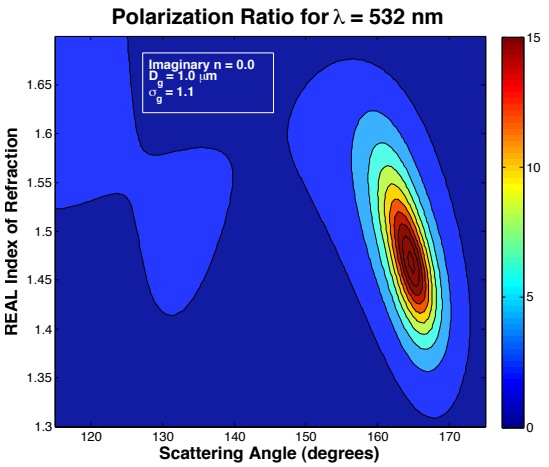

(a) Real Index

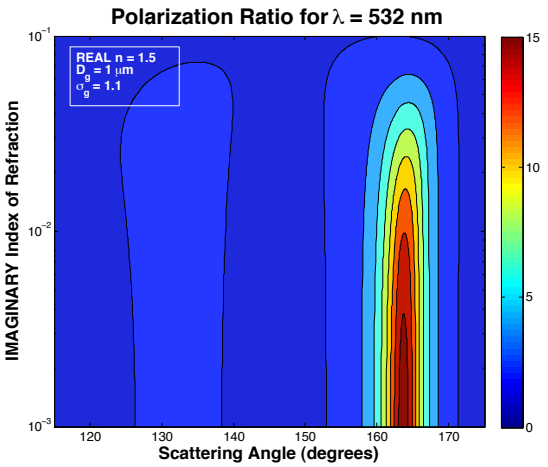

(b) Imaginary Index

Figure 6. Contours show how the polarization ratio magnitude changes as real refractive index (a) and the imaginary refractive index (b) change. Both sub-figures represent a single type of aerosol distribution with one micron diameter and a standard deviation of 1.1. The contribution of molecular scatter is not included in these polarization ratios.

This study assumes the index of refraction is fixed to emphasize the effect of concentration and size distribution characteristics on the polarization ratio. The sensitivity to the size distributions can be seen in Figures 7(a) and 7(b), where the overall effect of the aerosol size distribution on the polarization ratio is plotted as a function of scattering angle.

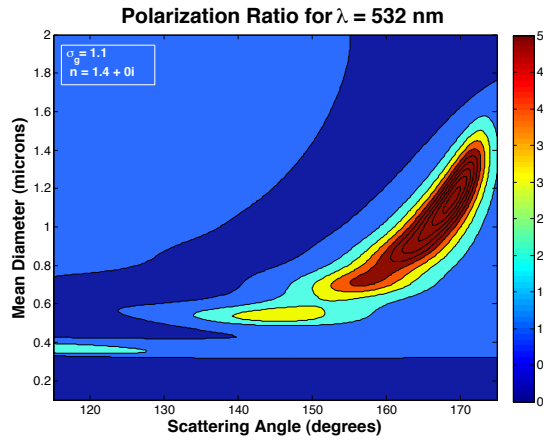

(a) Mean Diameter, D_g

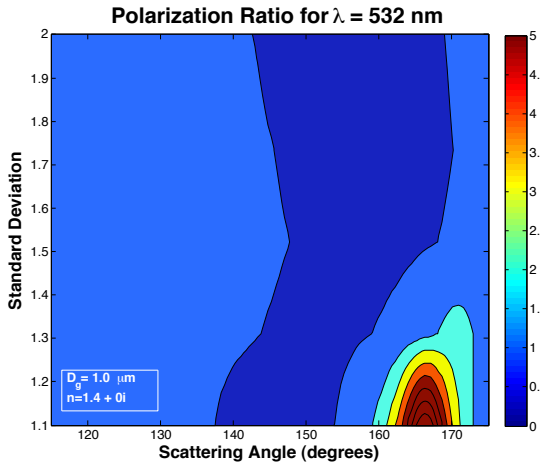

(b) Standard Deviation, σ_g

Figure 7. The mean diameter (a) and standard deviation (b) of the distribution effect on the polarization ratio. Contours represent the changing magnitude of the polarization ratio. These were calculated with only the aerosol contribution, no molecular background scattering.

Equation 1 expresses the fact that the polarization ratio includes scattering intensity from the volume containing aerosols and molecules. The scattering is dominated by the aerosols if their concentration is high, or by the molecular scattering if the aerosol concentration is low. Since 405 nm is the shortest wavelength, it will be the most sensitive to the changes in aerosol concentration, as seen in Figure 8.

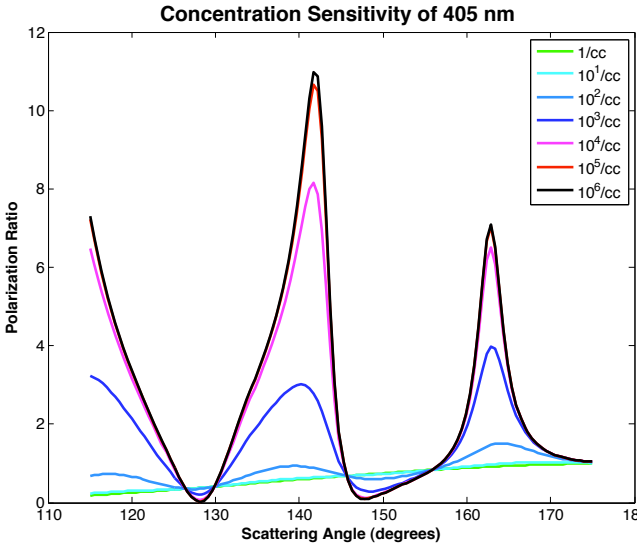

Figure 8. Concentration sensitivity of 405 nm wavelength.

Figure 8 shows calculations of scattering from a distribution of 1 micron diameter PSL aerosols. The refractive index used is $n = 1.61 + 0.0001i$, size distribution width is $\sigma_g = 1.01$, and mean diameter is $D_g = 1.0\mu m$. This case represents a lognormal size distribution strongly peaked around the mean diameter of one micron. An atmospheric lognormal size distribution is generally described by a geometric mean diameter, D_g, standard deviation, σ_g, and is described below.

$$\frac{dN}{dlog(D_p)} = \frac{N}{\sqrt{2\pi}\log_{10}(\sigma_g)} \exp\left(\frac{-(\log_{10}(D_p) - \log_{10}(D_g))}{2\log_{10}^2(\sigma_g)}\right) \tag{2}$$

where N is the number concentration and D_p is the diameter size bin width.[3]

Images that represent the intensity scattered as a function of angle for incident light polarized parallel and perpendicular to the scattering plane are analyzed. The intensity scattered at each angle is used to form the measured polarization ratio, $I_{||}/I_{\perp}$.

The theoretical polarization ratios are calculated using Mie phase functions as in Equation 1. The phase functions for a range of sizes are pre-calculated then summed by size distribution (as in Equation 1). The function is multiplied by the concentration and added to the intensity contributed by molecular scattering for each polarization and then the ratio is taken. This polarization ratio is compared to the experimentally determined polarization ratio. The calculated phase functions are for one particle, the sum over the size distribution takes care of the distribution of aerosol sizes, so it is an averaged phase function corresponding to the size distribution. The measured intensity is a sum of the phase functions of the particles within the element of the scattering volume with all the experimental factors, such as the optical efficiency included. However, by taking the ratio essentially all the experimental factors are canceled because they are identically present in each polarization.

The size distribution (mean diameter and standard deviation) and concentration are found by matching a calculated polarization ratio to the experimentally obtained ratio . These three parameters are calculated in the continuous genetic algorithm (CGA) by a *chromosome*, which represents a random possible solution. The chromosome in this case is made up of a string of three randomly generated numbers between 0 and 1, non-inclusive, each representing one of the three parameters. A sample chromosome is shown below.

$$\underbrace{0.8147}_{D_g}\ \underbrace{0.9058}_{\sigma_g}\ \underbrace{0.1270}_{N} \tag{3}$$

To relate this chromosome to the problem each piece of the chromosome must be mapped to the solution space for each parameter, see Table 1.

Table 1. A random number, r, is generated in the piece of the chromosome that represents each parameter and mapped to the parameter's solution space, between the input min and max values.

Parameter	**Minimum**	**Maximum**	**Mapping**
Mean Diameter (D_g)	0.002 μm	4 μm	$\mu_g(s) = r * (4 - 0.002) + 0.002$
Standard Deviation (σ_g)	1.01	1.80	$\sigma_g(s) = r * (1.80 - 1.01) + 1.01$
Number Concentration (N)	$10^{-2}\#/cc$	$10^{6}\#/cc$	$N(r) = r * (10^{3} - 10^{-2}) + 10^{-2}$

The inversion process uses the fixed value of refractive index for polystyrene latex(PSL). The refractive index used at each wavelength is shown in Table 2.

Table 2. The index of refraction values for PSL spheres.[8]

Wavelength [λ(nm)]	Index of Refraction [n]
405	1.61 + 0.001i
532	1.59 + 0.001i
655	1.58 + 0.001i

Figures 9(a) and 9(b) show the difference in polarization ratio for one micron diameter PSL spheres with different concentrations. The polarization ratios have a similar shape for both concentrations; however, the higher concentration shows slightly more structure from the aerosols.

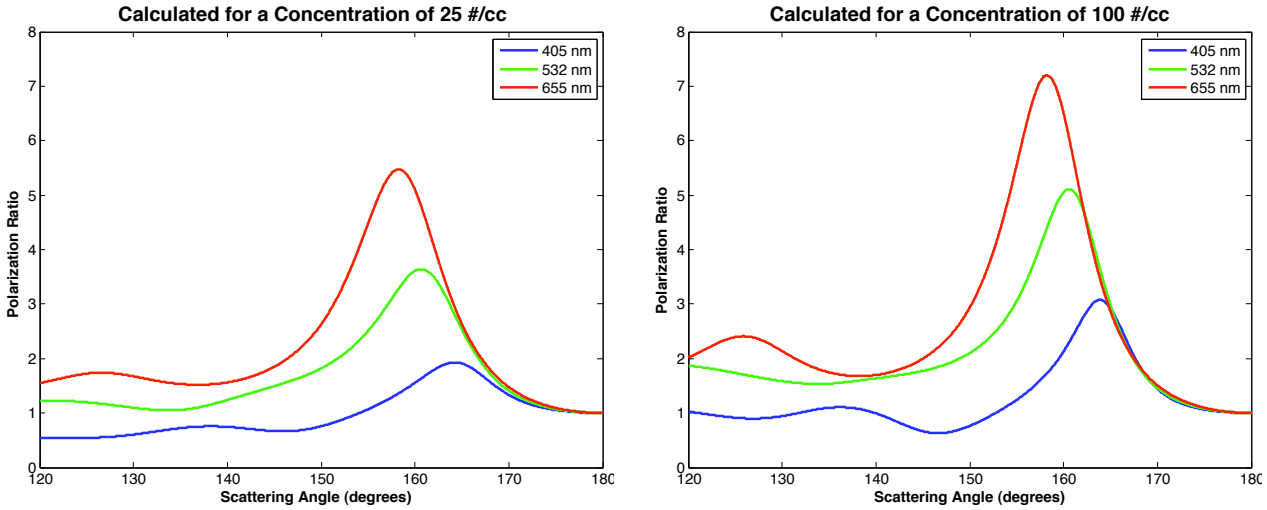

(a) Concentration of 100 #/cc

(b) Polarization Ratios

Figure 9. The calculated polarization ratios for the three wavelengths with a concentrations of 100 #/cc and 25 #/cc, for a standard deviation of 1.1.

4. ONE MICRON AEROSOL MEASUREMENTS

This experiment was performed at the Aerosol Chamber at John Hopkins Applied Physics Laboratory in August 2010. One micron polystyrene latex (PSL) spherical aerosols were released by a 24-jet collision nebulizer. Once released they mixed in the chamber by a fan until the aerosols reached a significant concentration. At that point, the nebulizer and fan were turned off. An APS was located at the floor of the chamber, about one meter below the visible beam to provide a real-time measurement of concentration, shown in Figure 10.

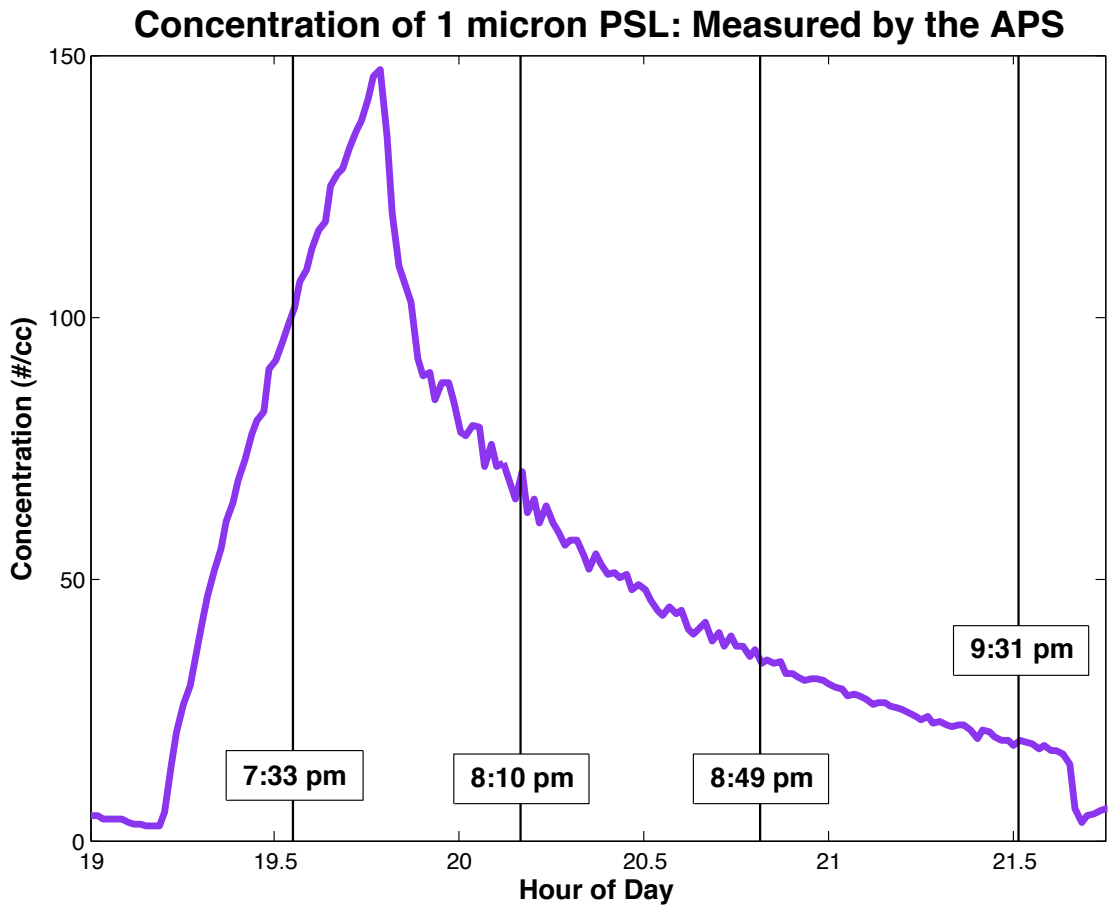

Figure 10. The total concentration measured by the APS in the APL aerosol chamber during the one micron diameter aerosol experiment. Times when data was taken by the mulitstatic multiwavelength instrument are represented by vertical lines.

Measurements made by the multiwavelength multistatic instrument are shown in Figures 11 -14. The comparison of sizes measured by the APS and calculated from the Continuos Genetic Algorithm (CGA) inversion of the polarization ratio measured by the multistatic multiwavelength instrument are shown in Tables 3 - 6 The polarization ratio calculated by the size distribution measured by the APS and the inversion of the data by the Continuous Genetic Algorithm are compared to the scattering measurements taken. The size distribution obtained by each method is also compared. The tables show the percent difference between each method of measurement.

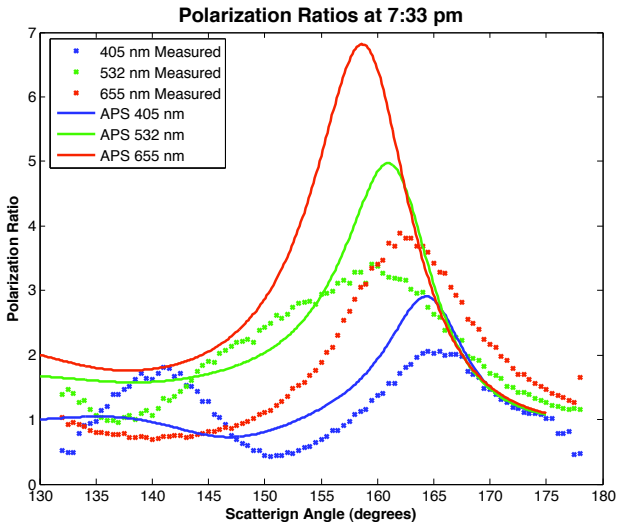

(a) Polarization Ratios

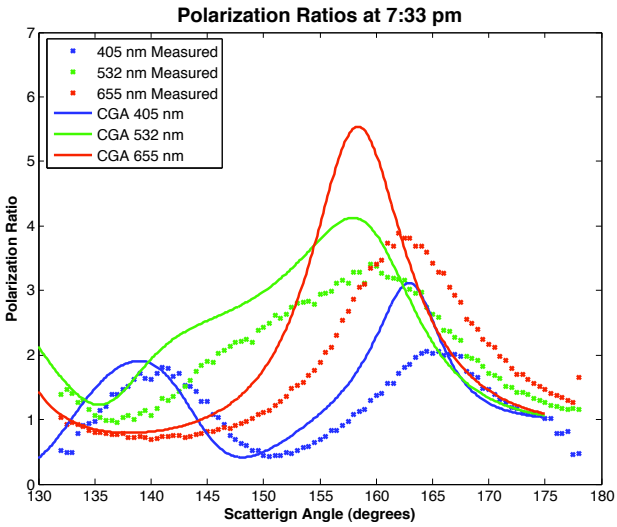

(b) Polarization Ratios

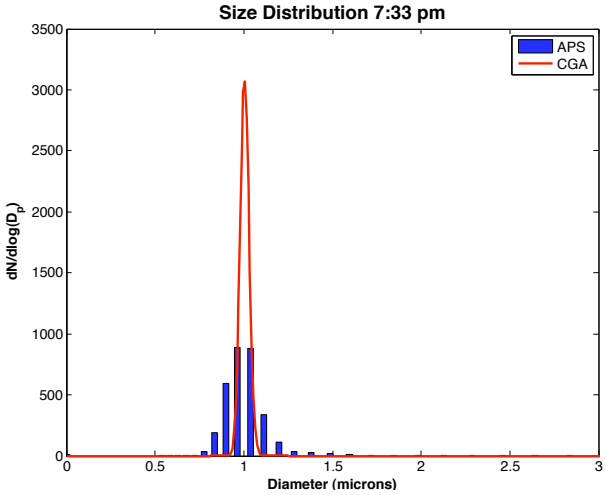

(c) Size Distribution

Figure 11. The calculated polarization ratio using the APS size distribution (a) and the calculated polarization ratio based on the CGA inversion routine (b) are compared with the measured data. The size distribution obtained by the APS and the CGA inversion routine are shown in (c).

Table 3. Comparison of Aerodynamic Particle Sizer (APS) and multistatic multiwavelength optical scattering instrument using a Continuous Genetic Algorithm (CGA) inversion routine.

	Mean Diameter, D_g (microns)	**Standard Deviation, σ_g**	**Concentration [#/cc]**
APS	1.00559	1.1365	101.842
CGA	1.0044	1.0221	84.9143
Difference	0.12 %	10.60 %	18.13 %

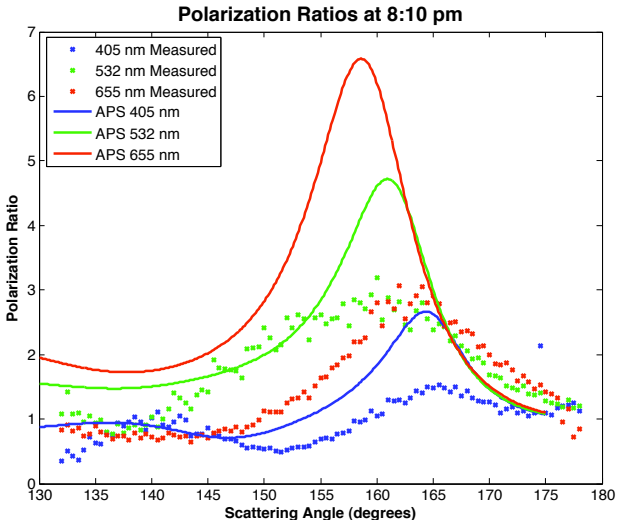

(a) Polarization Ratios

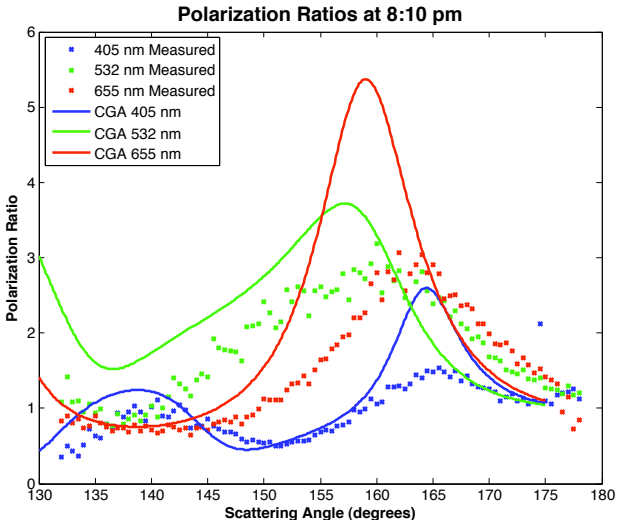

(b) Polarization Ratios

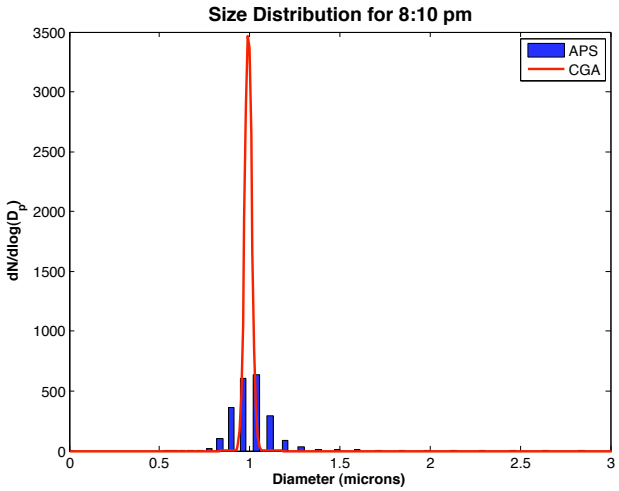

(c) Size Distribution

Figure 12. The calculated polarization ratio using the APS size distribution (a) and the calculated polarization ratio based on the CGA inversion routine (b) are compared with the measured data. The size distribution obtained by the APS and the CGA inversion routine are shown in (c).

Table 4. Comparison of Aerodynamic Particle Sizer (APS) and multistatic multiwavelength optical scattering instrument using a Continuous Genetic Algorithm (CGA) inversion routine.

	Mean Diameter, D_g (microns)	**Standard Deviation, σ_g**	**Concentration [#/cc]**
APS	1.00712	1.13086	70.4626
CGA	0.99194	1.0201	76.1317
Difference	1.52 %	10.30 %	7.73 %

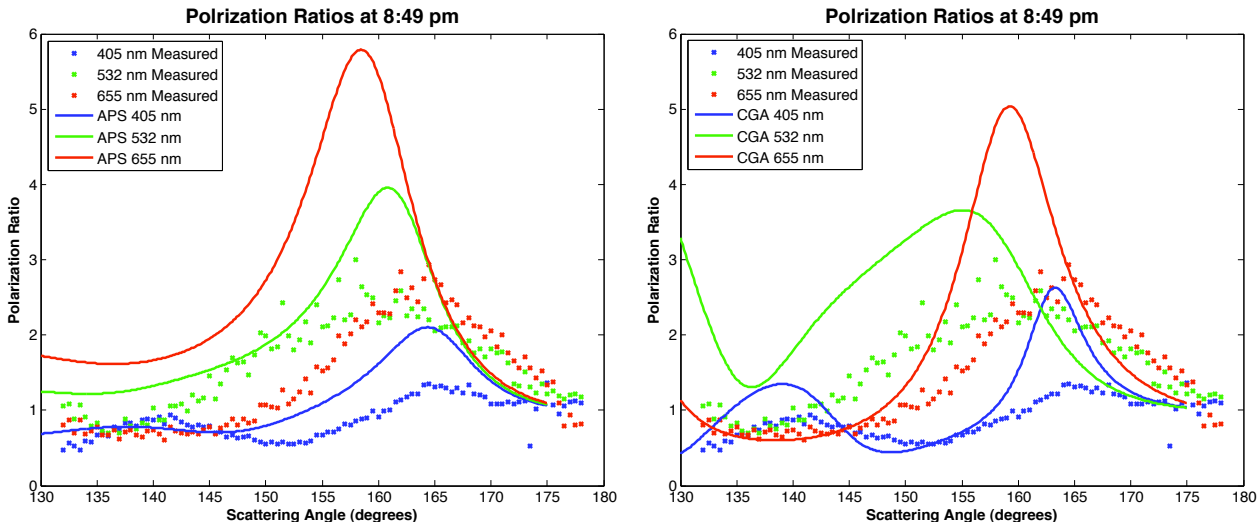

(a) Polarization Ratios

(b) Polarization Ratios

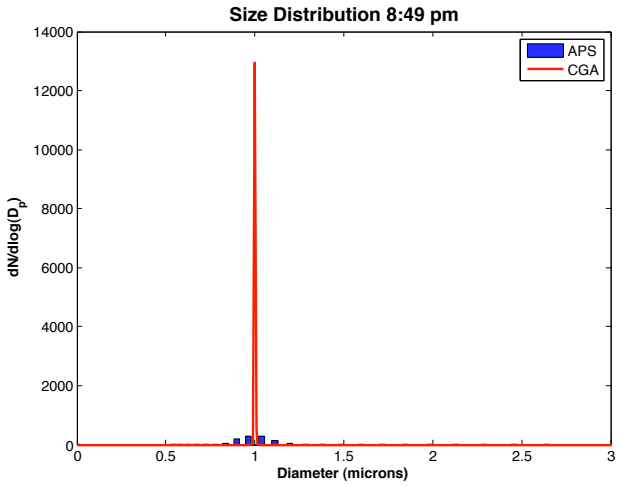

(c) Size Distribution

Figure 13. The calculated polarization ratio using the APS size distribution (a) and the calculated polarization ratio based on the CGA inversion routine (b) are compared with the measured data. The size distribution obtained by the APS and the CGA inversion routine are shown in (c).

Table 5. Comparison of Aerodynamic Particle Sizer (APS) and multistatic multiwavelength optical scattering instrument using a Continuous Genetic Algorithm (CGA) inversion routine.

	Mean Diameter, D_g (microns)	**Standard Deviation, σ_g**	**Concentration [#/cc]**
APS	0.99643	1.12881	33.8393
CGA	0.99928	1.003	47.8865
Difference	0.29%	11.81 %	34.38 %

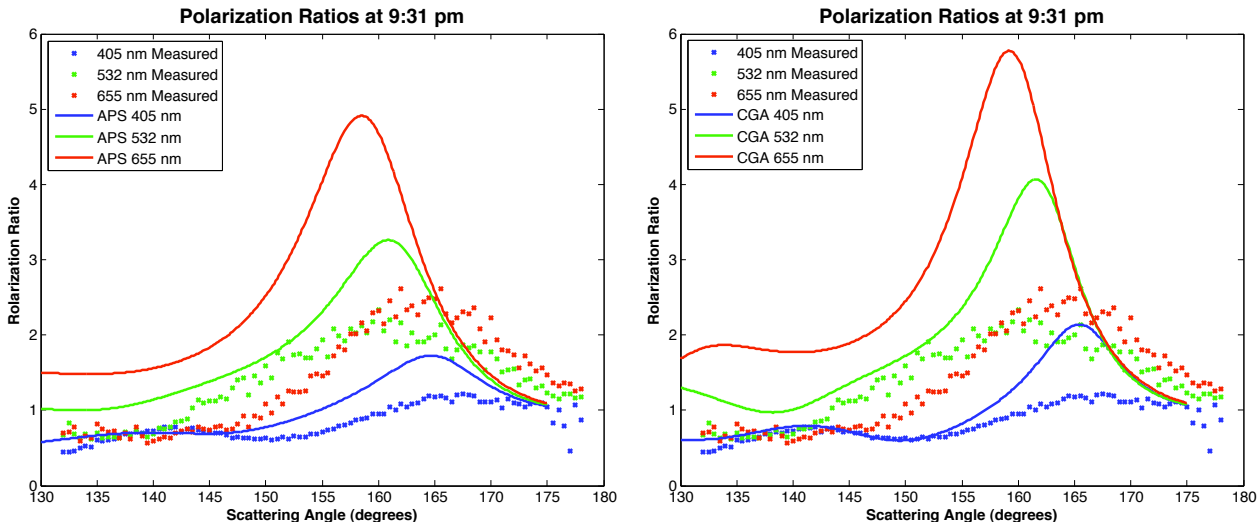

(a) Polarization Ratios

(b) Polarization Ratios

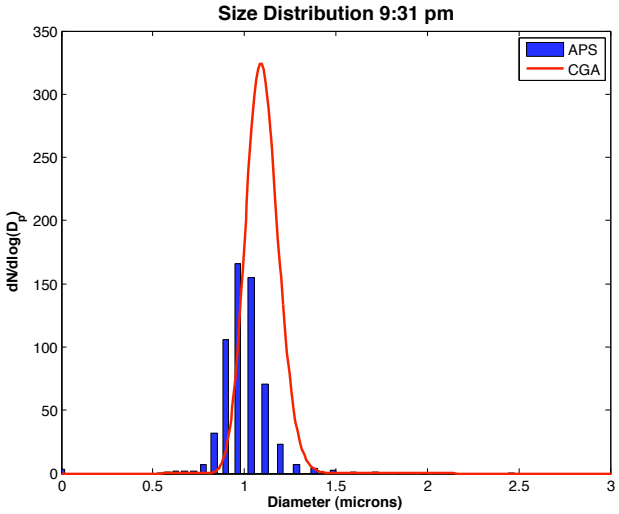

(c) Size Distribution

Figure 14. The calculated polarization ratio using the APS size distribution (a) and the calculated polarization ratio based on the CGA inversion routine (b) are compared with the measured data. The size distribution obtained by the APS and the CGA inversion routine are shown in (c).

Table 6. Comparison of Aerodynamic Particle Sizer (APS) and multistatic multiwavelength optical scattering instrument using a Continuous Genetic Algorithm (CGA) inversion routine.

	Mean Diameter, D_g (microns)	**Standard Deviation, σ_g**	**Concentration [#/cc]**
APS	0.998891	1.12483	18.9956
CGA	1.08882	1.0829	28.131
Difference	8.62 %	3.80%	38.77 %

Discrepancies between the polarization ratio method and the APS measurements are under investigation. The differences are most likely due to the fact that this is a highly nonlinear inversion. The polarization ratio is affected greatly by the standard deviation of the size distribution and the index of refraction of the aerosols, as shown in Figures 6(a), 6(b), 7(a) and 7(b), . The PSL spheres used in this experiment had a dye added to

make them fluoresce in the green and blue wavelength range when exposed to UV light. The 405 nm wavelength in the visible transmitter was within the absorption band for this dye, so the actual index of refraction for the blue wavelength may have a higher imaginary component. The effect of this higher absorption on the polarization ratio is show in Figure 15. In addition, the measured blue and green intensities may be effected by the fluorescence output by this dye. The polarization ratios observed compared to those predicted by the inversion results indicate little effect of the imaginary index to the polarization ratio. In this study the absorption of the 405 nm wavelength and the possible fluorescence intensity in the 405 nm and 532 nm wavelengths has been ignored.

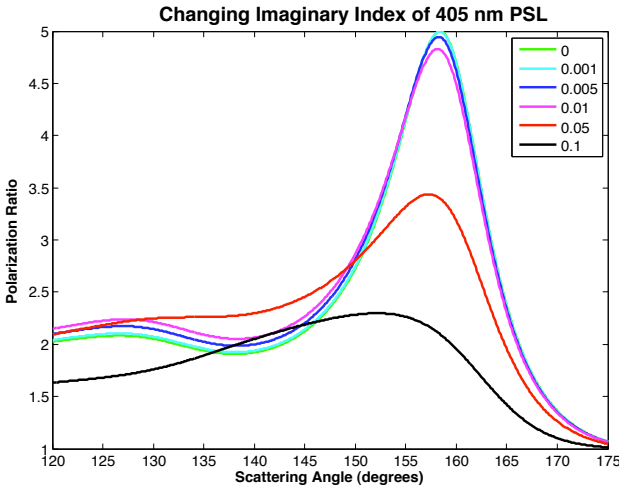

Figure 15. The polarization ratio associated with changes in the imaginary index of the one micron diameter PSL spheres.

5. CONCLUSIONS

The concentration of aerosols change the magnitude and structure of the polarization ratio as the concentration relative to the molecular background. This is seen in the measured polarization ratios while a chamber was filled with one micron diameter polystyrene spheres. The concentration and size distribution was measured by an Aerodynamic Particle Sizer and by the mulitwavelength multistatic instrument under development. The size distribution measured by the APS and determined using the multistatic multiwavelenth instrument show good agreement in the size distribution measured, but show discrepancies in the number concentration. However, both show an overall settling out of the aerosols as the concentration decreases following the maximum concentration. The measured polarization ratio shows better agreement with inversion results using a continuous genetic algorithm, than the calculated ratio from the size distribution measured by the APS. This conclusion is apparent when the aerosol concentrations are higher, early in the measurements described, see Figure 11. The multistatic, multiwavelength instrument is under development to characterize aerosols and determine their concentration in a large volume. This volume path averaged measurement determined by the inversion routine to predict the aerosol size distribution and number concentration should provide a more accurate volume description than the point measurement given by the APS.

5.1 Acknowledgments

The authors would like to thank Evan Thrush of the John Hopkins University Applied Physics Laboratory (JHU/APL) for partial funding of this research. A special thank you to Jason Quizon for his guidance in operating the JHU/APL aerosol chambers control and aerosol generation systems, and to David M. Brown for his assistance and direction with the data collection.

REFERENCES

[1] Bohren, C. F. and Huffman, D. R., [*Absorption and Scattering of Light by Small Particles*], WILEY-VCH Verlag GmbH & Co. KGaA, Weinheim (2004).

[2] Born, M. and Wolf, E., [*Principle of Optics*], Pergamon Press, New York (1980).
[3] Novitsky, E. J., *Multistatic Lidar Profile Measurements of Lower Tropospheric Aerosol and Particulate Matter: Multiple Scattering Measurements using Multistatic Lidar*, PhD dissertation, Pennsylvania State University, Department of Electrical Engineering (May 2002).
[4] Stevens, T. D., *Bistatic Lidar Measurements of Lower Tropospheric Aerosols*, PhD dissertation, Pennsylvania State University, Department of Electrical Engineering (May 1996).
[5] Park, J. H., *Multiple Scattering Measurements Using Mutistatic Lidar*, PhD dissertation, Pennsylvania State University, Department of Electrical Engineering (May 2008).
[6] Brown, A. M., *Multiwavelength Multistatic Optical Scattering For Aerosol Characterization*, PhD dissertation, Pennsylvania State University, Department of Electrical Engineering (Aug. 2010).
[7] Andrea M. Brown, M. G. S., Brouwer, L., and Philbrick, C. R., "Atmospheric aerosol characterization using multiwavelength multistatic light scattering," in [*Society of Photo-Optical Instrumentation Engineers (SPIE) Conference Series*], *Society of Photo-Optical Instrumentation Engineers (SPIE) Conference Series* **7684** (apr 2010).
[8] Ma, X., Lu, J. Q., Brock, R. S., Jacobs, K. M., Yang, P., and Hu, X.-H., "Determination of complex refractive index of polystyrene microspheres from 370 to 1610 nm," *Phys. Med. Biol.* **48**, 4165–4172 (2003).